Two Paradigms of Spatiotemporal Chaos: Spirals in Convection and Waves on Biomembranes

Markus Hilt, Werner Pesch, Walter Zimmermann

Two Paradigms of Spatiotemporal Chaos:
Spirals in Convection and Waves on Biomembranes

Markus Hilt[1], Werner Pesch[2], and Walter Zimmermann[1]

[1] Theoretische Physik, Universität des Saarlandes, 66041 Saarbrücken, Germany
E-mail: {mhilt, wz}@lusi.uni-sb.de
[2] Theoretische Physik, Universität Bayreuth, 95440 Bayreuth, Germany
E-mail: werner.pesch@uni-Bayreuth.de

We analyze two different systems, which show spatio–temporal chaos. One is spiral–defect chaos (*SDC*) in thermal convection, a well established complex pattern, which competes with stationary convection rolls near onset of convection. A quite simple two–dimensional model for SDC is provided by (generalized) Swift–Hohenberg (*SH*) equations, which are extensively used in the literature for many other systems as well. In particular we concentrate on the impact of spatially periodic modulations of the main control parameter, which leed to a transition from rolls to rectangles and in some cases to an interesting coexistence between stripes and defect chains. As a byproduct we describe a certain coarsening process of SDC towards a few big spirals for long–time SH-simulations. This is in contrast to experiments and rigorous solutions of the standard Boussinesq equations for convection and insinuates possible limitations of the SH-model. Our second pattern forming example addresses the dynamics of ionic channels in biomembranes. For their description we propose a novel model, which captures a Hopf bifurcations in systems with conserved quantities and which shows in fact surprising dynamical coarsening phenomena and spatio–temporal chaos.

1 Introduction

Applying sufficient stress to a system in a uniform state, for instance by a temperature or a density gradient, will often result in spatial or temporal patterns[1]. In particular striped patterns are ubiquitous in nature and are found in physical, chemical, and biological systems[1,2]. The analysis of the communality between the patterns and the understanding of universal aspects of pattern formation has been significantly promoted by the analysis of two–dimensional model equations like the various types of Ginzburg–Landau and Swift–Hohenberg (*SH*) equations[1,3,4]. Their formulation reflects the spatial and temporal symmetries of the underlying systems and some gross features of the pattern forming mechanism. While the patterns are typically well-ordered close to the bifurcation they reveal increasing spatio-temporal complexity when moving into the nonlinear regime. The goal of this paper is to exemplify the various types of such complex patterns in two different systems, which are both amenable to a description by 2d-models.

We will at first consider convection in a horizontal fluid layer heated from below, known as Rayleigh-Bénard convection (*RBC*), which is one of the best studied examples of pattern forming systems[1,5,6]. Beyond a critical temperature difference between the bottom and top boundary of the convection cell shown in Fig. 1, convection rolls occur. Cold and warm regions alternate periodically at the upper surface. They are optically visualized as a 2d-striped pattern by exploiting the temperature dependence of the refraction index. The resulting intensity modulations are considered as an order parameter. The system is dissipative (heat diffusion, viscous flow) and the standard model equations resemble generalized (nonlinear) diffusion equations.
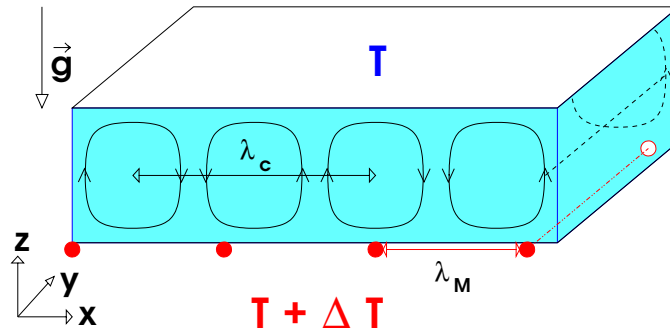
Figure 1. A sketch of a thermal convection cell. Beyond a critical temperature difference ΔT between the lower and the upper container boundary convection rolls bifurcate from the heat conducting state. The temperature difference may be also spatially periodic modulated with a modulation wavelength λ_m, as indicated by the read heat wires.

The fully rigorous three-dimensional description of thermal convection rests upon the Boussinesq equation. One obtains in fact stable roll solutions in a fairly large regime of the applied temperature gradient to the fluid layer and wavenumber of the roll patterns (the "Busse balloon")[1,5]. Therefore, the recent observation of spiral–defect chaos (SDC) in a parameter regime where it competes with the stable roll attractor was rather surprising[7,8]. The complex spatio–temporal dynamics of SDC involves rotating spirals, targets, dislocations etc. that have been modeled first by numerical simulations of so–called generalized Swift–Hohenberg (*SH*) equations[9–12]. These simulations provided important insights into the underlying mechanism of SDC, however, the generalized SH model implies approximations with possible limitations. Therefore, the reliability and the range of validity of 2d-models for RBC is of considerable interest. A check of such models against rigorous results is possible, because most of the characteristic properties of SDC are reproduced with high precision by the standard Boussinesq equations[13–15]. In fact the long–time dynamics of solutions of the SH equation, which is characterized by small spirals coalescing into a few big ones[16], is in contrast to the experiments and rigorous Boussinesq solutions (see Sec. 2.1).

In addition we will take the opportunity to investigate the impact of spatial modulations of the control parameter on SDC (see Sect.2.2). We will show that in this case rolls can be substituted by rectangles at threshold. Further above threshold instead of SDC defect chains become favored against SDC. These features seem to be generic, since they are observed in the modulated generalized SH model and the modulated Boussinesq equations as well[17].

As a second example we will study in Sect. 3 the dynamics of interacting ion–channels in biomembranes[18]. Their activity (measured at the outer 2d surface of the membrane) can also display patterns that may vary in space and time. The fact, that the number of ion channels is fixed, gives rise to a "conserved" order parameter, in contrast to the "non-conserved" order parameter ($\equiv$ temperature field in RBC), and requires substantially different types of models. Thus, to describe the ion–channel dynamics we have constructed a novel universal model equation for a conserved order parameter. They lead to complex spatio-temporal patterns and coarsening mechanism, which differ substantially from those observed in the complex Ginzburg-Landau equation[19–21], which is used as the universal description of waves (Hopf-bifurcations) in the case of an unconserved order parameter.

2 Spiral-Defect Chaos and its Modulations

In this section we discuss simulations of the generalized SH–equations in a parameter range where SDC occurs. In this model the two real fields $\psi(\mathbf{r}, t)$ and $\zeta(\mathbf{r}, t)$ (see e.g.Ref. 9, 10) are coupled and we allow also a modulation of the control parameter by a spatially periodic function $M(x) = 2G\cos(kx)$ with $k = 2\pi\lambda_M$,

$$\Big[\partial_t + g_m \mathbf{U} \cdot \nabla\Big]\psi = \Big[\varepsilon + M(x) - (1 + \Delta)^2\Big]\psi - \psi^3, \qquad (1a)$$

$$\Big[\tau_\zeta \partial_t - \mathcal{P}(\eta\nabla^2 - c^2)\Big]\Delta\zeta = \Big[(\partial_y\psi)\partial_x - (\partial_x\psi)\partial_y\Big]\Delta\psi. \qquad (1b)$$

$\psi(\mathbf{r}, t)$ describes the planar spatial variations of convection patterns (e.g. the temperature field), which consist locally of convection-roll patches. $\zeta(\mathbf{r}, t)$ is a velocity potential determining the mean flow $\mathbf{U} = (\partial_y\zeta, -\partial_x\zeta)$. The control parameter $\varepsilon = 2.78\,(\Delta T - \Delta T_c)/\Delta T_c$ serves as a dimensionless measure for the applied temperature difference ΔT across the fluid layer. The time is scaled in such a way that a time lapse of $t = 5$ in Eqs. (1) corresponds to the common vertical diffusion time t_v, which is about a few seconds in experiments.

Any curvature of the rolls produces a vertical vorticity field $-\Delta\zeta(\mathbf{r}, t)$ which increases with decreasing Prandtl number $\mathcal{P}$ according to Eq. (1b). In contrast to the claims expressed in several papers by Gunton and coworkers (see e.g. Ref. 25), only the dominant term $\sim c^2$ on the left-hand side of Eq. (1b) can be directly traced back to the Boussinesq equations. The two other terms $\propto \tau_\zeta, \eta$, respectively, are in principle phenomenological, as discussed in some detail in Ref. 11. In Eq. (1a) the relevance of $\zeta(\mathbf{r}, t)$ is controlled by the coupling constant g_m. The value of g_m can be calculated as $g_m = 12.2$ for $c^2 = 2$ and $\mathcal{P} = 1$ by comparison with the known zig-zag stability boundary of convection rolls[22].

The coupling to the mean flow, which becomes more important either at small $\mathcal{P}$ or large g_m is crucial for persistent SDC. In the limit of large Prandtl numbers $\mathcal{P}$, where ζ is hardly excited, the dynamics of ψ becomes purely relaxational and approaches a low dimensional stationary state of the corresponding Lyapunov functional.[1,4] Note, however, that any strongly disordered pattern before it equilibrates generates virtually instantaneously a strong, long-range mean-flow $\mathbf{U}$ according to Eq. (1b) and can thus easily lead to a transient SDC-like dynamics.

2.1 Coarsening of SDC

In our numerical solutions of Eqs. (1) without modulations ($M(x) = 0$) we have chosen the same set of parameters as in the previous works[9, 10, 25], namely $c^2 = 2$, $g_m = 50$, $\tau_\zeta = \eta = \mathcal{P} = 1$, $\varepsilon = 0.7$. Mostly we consider an aspect ratio of $\Gamma = L/2d = 32$ where L denotes the lateral extension of the convection cell and d its thickness. At first we have performed simulations in a square domain with periodic boundary conditions in order to avoid an artificial bias from the sides. Starting from random initial conditions yields a typical snapshot as shown in Fig. 2(a) at $800t_v$. This pattern compares well with those already shown in Refs. 9, 10 at the same time lapse. It resembles also the characteristic SDC snapshots observed persistently in experiments[7,8] or during numerical solutions of the fundamental Boussinesq equations[13]. However, when continuing the runs over much longer periods beyond $8000t_v$ the scenario changes qualitatively and the pattern coarsens
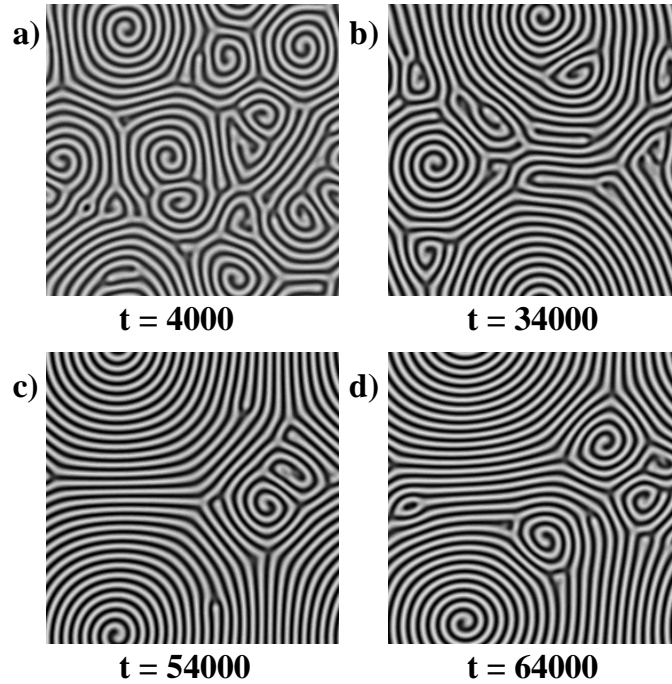
Figure 2. The the two dimensional solution $\psi(\mathbf{r}, t)$ of (1) for periodic boundary conditions is plotted at increasing times t after starting with random initial conditions[16]. The parameters are $\Gamma = 32$ (aspect ratio), $\varepsilon = 0.7$, $g_m = 50$, $c^2 = 2$, $\eta = 1$, $\mathcal{P} = 1$ and $\tau_\zeta = 1$.

towards a "big spiral" as shown in Fig. 2(c) and Fig. 2(d), which rotates about a slowly migrating center. Only at the boundaries of the big spiral one finds remnants of the previous persistent generation and annihilation of small spirals. For $\mathcal{P} \approx 1$ the coarsening to big spirals is neither observed in experiments nor during simulations of the Boussinesq equations. For more details about this coarsening we refer to 16, 26.

Though for many purposes generalized SH-models are certainly very valuable tools to study 2d-patterns, however, our investigations of SDC show clearly that one has to be aware that the long–time behavior of hydrodynamic systems might not be adequately modeled. Accordingly, their application to coarsening studies[27] or to the analysis of statistical properties of SDC[25] might be questionable.

2.2   Effects of a Spatially Modulated Control Parameter

Spatially periodic modulations of spatially periodic patterns can lead to commensurate–incommensurate transitions[28, 29] or to surprising two-dimensional patterns[30–32]. In other cases spatial periodic modulations break in addition the local reflection symmetry and induce time dependent patterns[33–35]. Spatial modulations of parameters may also be viewed as a control technique in some analogy to temporal controlling of unstable states in low dimensional temporal chaos[36, 37] or to the control of spatio-temporal complex phenomena[38, 39]. SDC is intrinsically quasi two–dimensional and of rather different nature than the
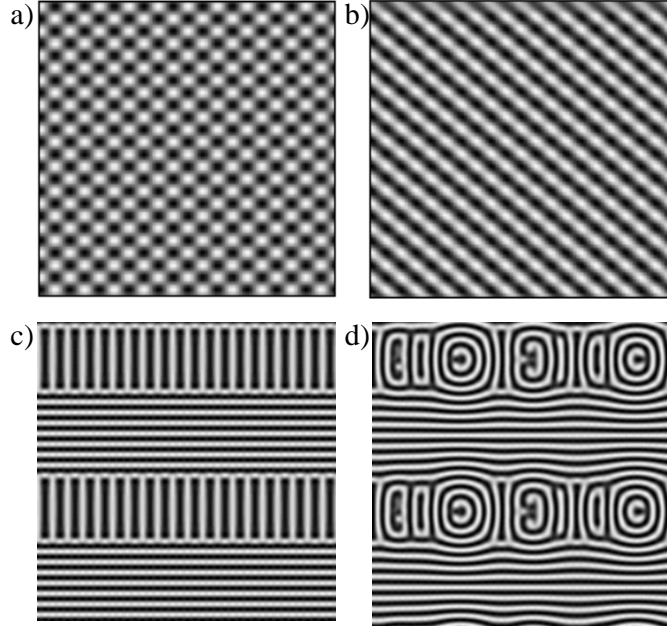
456

Figure 3. In a) a rectangular pattern is shown, that occurs at a forcing wavenumber $k = 5q_0/4$ and a forcing amplitude $G = 0.3$ immediately above threshold. Increasing the control parameter to $\varepsilon = 0.7$ a transition to modulated rectangles takes place as shown in part b). For a slightly smaller modulation $G = 0.2$ the solution as shown in c) is stable. When the modulation amplitude is further reduced to $G = 0.077$ the range of the vertical stripes becomes unstable against spiral formation.

examples mentioned before. Hence controlling or forcing of this experimentally accessible pattern is expected to lead to different and new phenomena.

The onset of pattern described by the model in Eqs. (1) is reduced from $\varepsilon_c = 0$ in the case without modulations to $\varepsilon_c = -2G$ with a finite modulation amplitude G and modulation wavenumber $k < 2q_0$. In this range the projection of the wavenumber $\mathbf{q}_0 = (q_x, q_y)$ of the pattern onto the x–axis is in $2:1-$resonance with the modulation wave number $2q_x = k$. Especially in the range $k \sim q_0$ rectangular pattern occur at threshold as shown in Fig. 3a) for $k = 5q_0/4$ and $G = 0.15$. If the control parameter is further increased beyond threshold a transition from rectangles to modulated rectangles takes place, c.f. Fig. 3b).

If the effect of mean flow is taken into account with the coupling constants $g_m = 50$ and $\mathcal{P} = 1$, again at threshold rectangles occur at first. However, increasing the control parameter up to $\varepsilon = 0.7$, where SDC occurs in the absence of modulations $M(x) = 0$, then one observes a transition from SDC to defect chains which are similar to the pattern shown in Fig. 3d). This coexistence between the horizontal stripe pattern and the SDC like pattern is due to an interplay between the mean flow field $\zeta(x, y)$ and the modulation $M(x)$. This interplay stabilizes for stronger modulations also the surprising coexistence of two orthogonal stripe pattern as shown for $G = 0.2$ in Fig. 3c). For a modulation amplitude of about $G = 0.07$ the vertical stripes shown in Fig. 3c) become unstable with respect to SDC like pattern as given in Fig. 3d). Also this surprising pattern persists forever. Close to the transition from a pattern shown in Fig. 3c) to a pattern as shown in Fig. 3d) the

457

embedded SDC like ranges are stationary. Reducing the amplitude G further, then the SDC like pattern becomes time dependent, but the narrow SDC like range in Fig. 3d) is still stable in some range of G. However, after a further reduction of G the SDC like stripes invade the range of the horizontal stripes and for $G \to 0$ SDC patterns are met everywhere as discussed in Sec. 2[40]. From simulations of the Boussinesq equations with a modulated temperature difference ΔT a very similar scenario is obtained, as described in more detail elsewhere[17].

3 Biomembranes

In a model describing the collective dissipative dynamics of ionic channels in biomembranes, an oscillatory bifurcation has been found[41]. Since the ion–channels are neither created nor annihilated, the ion–channel density is a conserved quantity. Therefore, the Hopf bifurcation in this system is rather different from common oscillatory systems[21], where the major fields are unconserved. Accordingly, the common complex amplitude equation with complex coefficients (see e.g. Ref. 1, 21), which describes the nonlinear solutions above an oscillatory instability in systems with unconserved quantities, cannot be applied to a description of the generic properties of the oscillating ion–channel density.

In a system with conserved fields, the equation for the complex order parameter field $A(x, y, t)$ beyond an oscillatory instability is as follows[18]

$$\partial_t A = -\nabla^2 \left(\eta + ia + (1+ib)\nabla^2 - (1+ic)|A|^2) \right) A$$
$$+(d_1 + id_2)\nabla \left[(A^*\nabla A - A\nabla A^*) A \right]. \tag{2}$$

This equation has been derived on the basis of general symmetry principles and conservation laws. Alternatively Eq. (2) has been derived from the basic equations of motion of the ionic–channels by a generalized perturbation expansion around the basic state[18]. In this case the coefficients can be expressed in terms of the diffusion constants, the charge and the mobility of the ion–channels.

The basic state $A = 0$ becomes unstable against small perturbations of the form $A \propto e^{\sigma t + iQx}$, if the growth rate $\lambda_A = \Re(\sigma(Q))$ becomes positive, with the complex dispersion

$$\sigma(Q) = Q^2(\eta + ia - (1+ib)Q^2). \tag{3}$$

The growth rate $\lambda_A(Q)$ takes its maximum at the wavenumber $Q_m = \sqrt{\eta/2}$. Starting a numerical simulation of Eq. (2) in one spatial dimension with random initial conditions, the Fourier mode corresponding to the wave number Q_m is indeed the fastest growing mode in the initial state as can be seen at the bottom of Fig. 4a). However, the saturated nonlinear right (left) traveling wave solutions $A = F \exp[i(\Omega t - (+)Q_m x)]$ of Eq. (2) are unstable with respect to modulations with a wavenumber K and the original traveling–wave solution even changes its propagation direction in most cases. At the same time the wavelength (wavenumber) increases (decreases) and the resulting coarsening process can be observed in the middle of the space–time plot of Fig. 4a). The resulting slightly modulated traveling wave exists for a quite long transient period (that is not fully shown) but it becomes again unstable with respect to a short wavelength instability, to be seen in the middle of Fig. 4b). In the late stage of the coarsening process the solution approaches always a traveling wave state with the largest possible wavelength set by the periodicity lenght L of the system (we
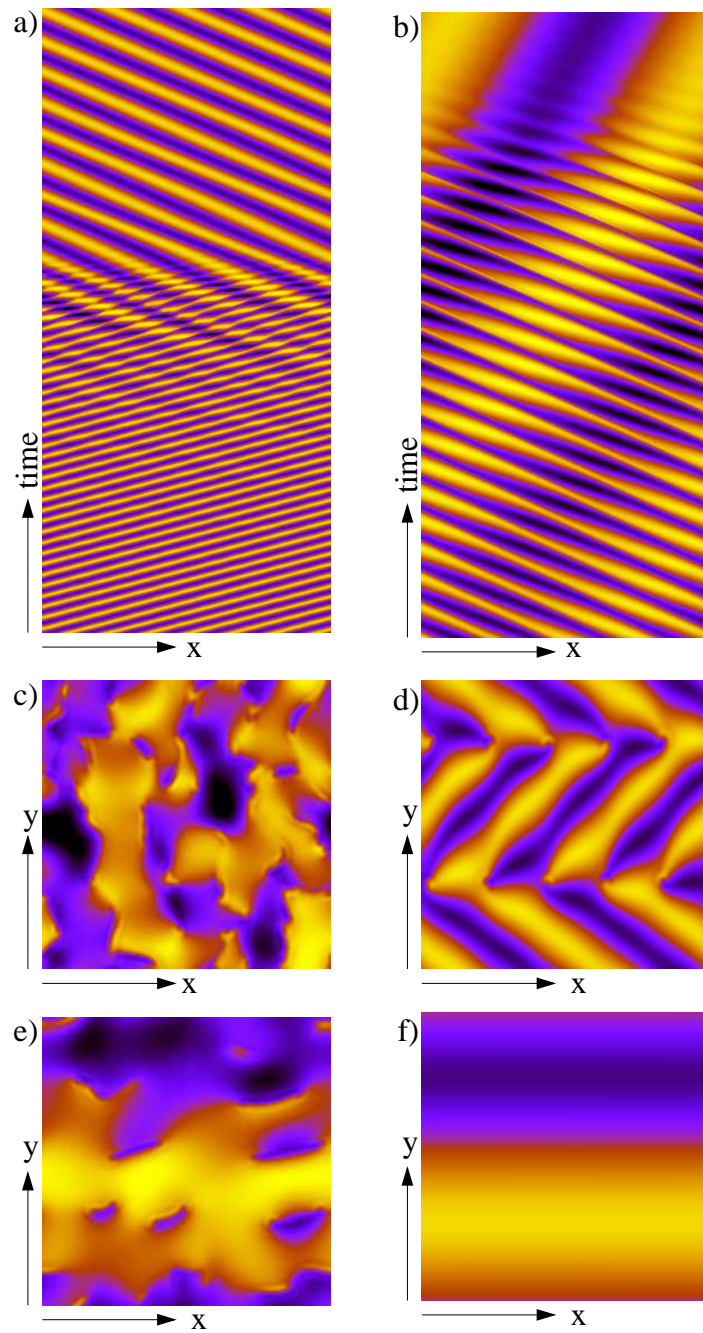
Figure 4. The real part $\Re(A(x,t))$ of a one-dimensional solution of Eq. (2) is shown as a space-time plot in panels a) (initial state), b) (later stage). The coarsening is obvious. The corresponding two-dimensional solutions are shown in panels c)-f) each at a fixed time. The following parameters in Eq. (2) have been used: $\eta = 1$, $a = 0.4$, $b = 1$, $c = -2$, $d_1 = 0.2$, $d_2 = -0.1$.

use periodic boundary conditions). If non-flux boundary conditions are used, the coarsening is essentially unchanged, but one has to deal with the opposite propagation direction of the traveling waves too.
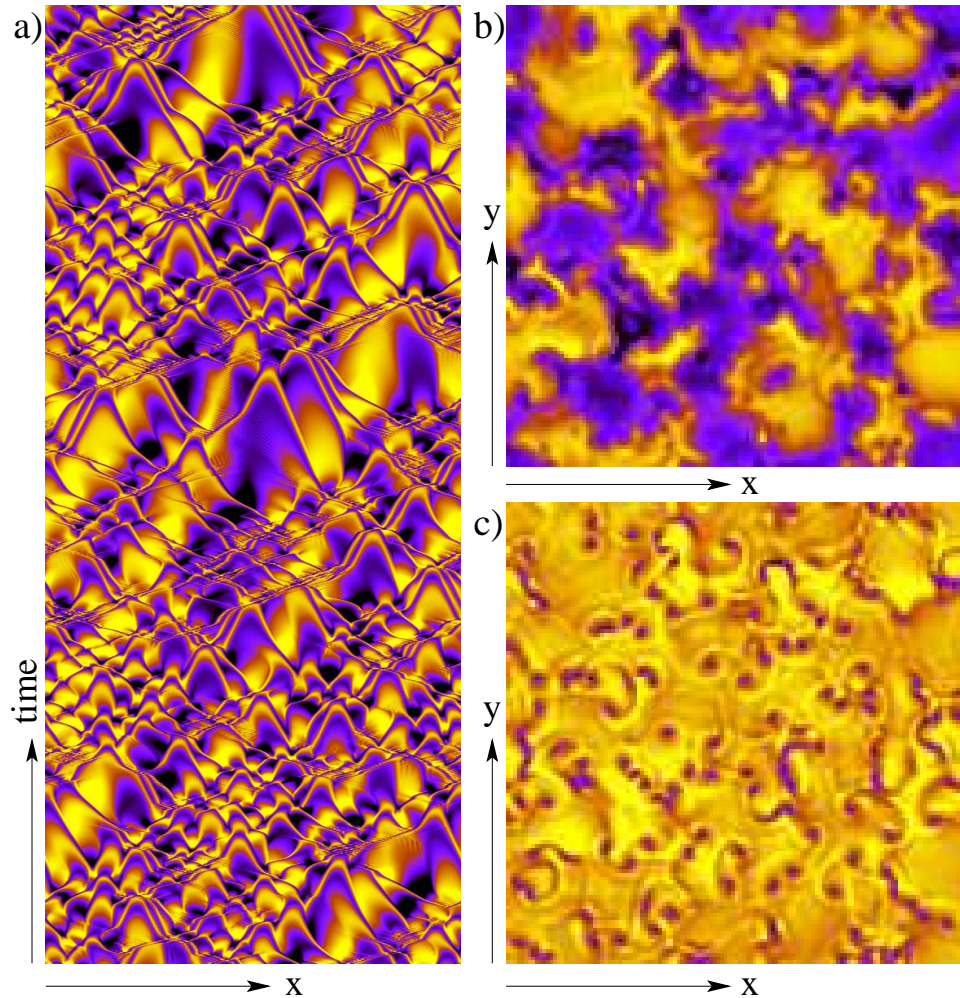

Figure 5. In a) the real part $\Re(A(x,t))$ of the one dimensional solution of Eq. (2) is shown. This is in a parameter regime with persistent spatio-temporal chaos. In b) the real part $\Re(A(x,y,t_0))$ of the two–dimensional solution is shown at a fixed time t_0 and in c) the modulus $|A(x,y,t_0)|$. The parameters for these simulations in Eq. (2) are $\eta = 1$, $a = 0.5$, $b = 1$, $c = -1.73$, $d_1 = 0.4$, $d_2 = 1.1$.

For the same parameters as in Fig. 4a) and in Fig. 4b) the coarsening process in two spatial dimensions is slightly different as indicated by Figs. 4c)-f). Fig. 4c) shows the real part of the solution at an intermediate time. Slightly afterward, similar as in Fig. 4d), very often a Zig-Zag like pattern occur, which itself becomes unstable after a longer transient period. During a further intermediate regime solutions similar as in Fig. 4e) occur, but finally also in two spatial dimensions the traveling wave state, as shown in Fig. 4f), is the

preferred state. This scenario holds for a large range of parameters in one and two spatial dimensions. This dynamical coarsening is rather different from the common coarsening phenomena[42, 27, 11] and more details will be described elsewhere. The duration of the whole coarsening process increases with the system size L.

There are also parameter regimes with persistent spatio-temporal chaotic solutions of Eq. (2). An example of this solution type in one spatial dimension is given by a space-time plot in Fig. 5a). In two spatial dimensions two snap shots of this solution at the same parameters are given in Fig. 5b) and Fig. 5c), where the real part $\Re(A(x,y)$ is shown in part b) and the modulus $|A(x,y)|$ in part c). The blue dots in Fig. 5c) correspond to zeros of the modulus $|A(x,y)|$ and therefore to defects of the complex field $A(x,y)$. A more complete characterization of these solutions is given elsewhere[18].

4 Conclusions

We have shown, that certain 2-d models are very useful to describe generic features of spatio-temporal complex patterns. Nevertheless one has to be aware of their possible short-comings. Forthcoming experiments (E. Bodenschatz, Cornell Univerity) are dedicated to test in particular our predictions regarding the influence of spatial modulations on SDC. This will certainly give rise to an interesting interplay between numerical and experimantal investigations. Our investigations of the new model for the dynamics of ion-channels have just started. In view of the intensive work on the complex Ginzburg-Landau equation for oscillatory patterns with a non-conserved orderparameter[21], certainly one of the most studied nonlinear equations in physics, and the applications to biophysics we are looking forward to intensive studies of our model as well.

Acknowledgments

References

1. M. C. Cross and P. C. Hohenberg. Pattern formation outside of equilibrium. *Rev. Mod. Phys.*, 65:851, 1993.
2. P. Ball. *The Self-Made Tapestry: Pattern Formation in Nature*. Oxford Univ. Press, Oxford, 1998.
3. A. C. Newell, T. Passot, and J. Lega. Order parameter equations for patterns. *Annu. Rev. Fluid Mech.*, 25:399, 1992.
4. J. B. Swift and P. C. Hohenberg. Hydrodynamic fluctuations at the convective instability. *Phys. Rev. A*, 15:315, 1977.
5. F. H. Busse. Fundamentals of thermal convection. In W. R. Peltier, editor, *Convection: Plate Tectonics and Global Dynamics*, pages 23–95, Montreux, 1989. Gordon and Breach.
6. E. Bodenschatz, W. Pesch, and G. Ahlers. Recent developments in rayleigh-bénard convection. *Annu. Rev. Fluid Mech.*, 32:709, 2000.

7. S. W. Morris, E. Bodenschatz, D. S. Cannell, and G. Ahlers. Spiral defect chaos in large aspect ratio Rayleigh–Bénard convection. *Phys. Rev. Lett.*, 71:2036, 1993.

8. M. Assenheimer and V. Steinberg. Transition between spiral and target states in Rayleigh-Bénard convection. *Nature (London)*, 367:345, 1994.

9. H. W. Xi, J. D. Gunton, and J. Vinals. Spiral defect chaos in a model of Rayleigh–Bénard convection. *Phys. Rev. Lett.*, 71:2030, 1993.

10. M. C. Cross and Y. Tu. Defect dynamics for spiral chaos in Rayleigh-Bénard convection. *Phys. Rev. Lett.*, 75:834, 1995.

11. M. C. Cross. Theoretical modelling of spiral chaos in Rayleigh–Bénard convection. *Physica D*, 97:65, 1996.

12. M. Bestehorn, M. Fantz, R. Friedrich, and H. Haken. Hexagonal and spiral patterns of thermal convection. *Phys. Lett. A*, 174:48, 1993.

13. W. Decker, W. Pesch, and A. Weber. Spiral defect chaos in Rayleigh–Bénard convection. *Phys. Rev. Lett.*, 73:648, 1994.

14. W. Pesch. Complex spatio-temporal convection patterns. *Chaos*, 6:348, 1996.

15. D. A. Egolf, I. V. Melnikov, W. Pesch, and R. E. Ecke. Mechanism of extensive spatiotemporal chaos in Rayleigh-Bénard convection. *Nature*, 404:733, 2000.

16. R. Schmitz, W. Pesch, and W. Zimmermann. Spiral Defect Chaos: Swift–Hohenberg equation versus Rayleigh-Bénard Convection. *Phys. Rev. E*, 65:037302, 2002.

17. W. Pesch and W. Zimmermann. Domain pattern and taming of spiral defect chaos in thermal convection. (unpublished), 2003.

18. M. Hilt and W. Zimmermann. About a Hopf-bifurcation in systems with conserved quantities and dynamical coarsening. (submitted), 2003.

19. K. Stewartson and J. T. Stuart. *J. Fluid Mech.*, 48:529, 1971.

20. A. C. Newell. Finite bandwidth finite amplitude convection. *Lect. Appl. Math.*, 15:157, 1974.

21. I. Aronson and L. Kramer. The world of the complex Ginzburg–Landau equation. *Rev. Mod. Phys.*, 74:99, 2002.

22. The coupling constant g_m depends weakly on the Prandtl number $\mathcal{P}$ in the vicinity of 1. Its relevance to the zig-zag instability is for instance discussed in Ref. 23, 24.

23. M. Cross, Phys. Rev. A **27**, 490 (1983).

24. W. Decker and W. Pesch, J. de Phys. (Paris) II, **4**, 419 (1994).

25. H. W. Xi and J. D. Gunton. Spatiotemporal chaos in a model of Rayleigh–Bénard convection. *Phys. Rev. E*, 52:4963, 1995.

26. R. Schmitz and W. Zimmermann. Spiral–defect chaos in a model of thermal convection: Long time dynamics. submitted, 2003.

27. M. C. Cross and D. I. Meiron. Domain coarsening in systems far from equilibrium. *Phys. Rev. Lett.*, 75:2152, 1995.

28. M. Lowe, B. S. Albert, and J. P. Gollub. Convective flows with multiple spatial periodicities. *J. Fluid Mech.*, 173:253, 1986.

29. P. Coullet. Commensurate-incommensurate transition in nonequilibrium systems. *Phys. Rev. Lett.*, 56:724, 1986.

30. P. Coullet, R.E. Goldstein, and G. H. Gunaratne. Parity-breaking transition of modulated patterns in hydrodynamics systems. *Phys. Rev. Lett.*, 63:1954, 1989.

31. W. Zimmermann, A. Ogawa, S. Kai, K. Kawasaki, and T. Kawakatsu. Wavelength competition in convective systems. *Europhys. Lett.*, 24:217, 1993.

32. A. Ogawa, W. Zimmermann, K. Kawasaki, and T. Kawakatsu. Forced periodic and quasi-periodic patterns in anisotropic systems. *J. Phys. II (Paris)*, 6:305, 1996.

33. G. Hartung, F. H. Busse, and I. Rehberg. Time–dependent convection induced by broken spatial symmetries. *Phys. Rev. Lett.*, 66:2741, 1991.

34. W. Zimmermann and R. Schmitz. Hopf bifurcation by frustrated drifts. *Phys. Rev. E*, 53:R1321, 1996.

35. R. Schmitz and W. Zimmermann. Spatially periodic modulated Rayleigh-Bénard convection. *Phys. Rev. E*, 53:5993, 1996.

36. E. Ott, C. Grebogi, and J. A. Yorke. Controlling chaos. *Phys. Rev. Lett.*, 64:1196, 1990.

37. T. A. Shinbrot. Progress in the control of chaos. *Adv. Phys.*, 44:73, 1995.

38. D. Auerbach. Controlling extended systems of chaotic elements. *Phys. Rev. Lett.*, 72:1184, 1994.

39. I. Aronson, H. Levine, and L. Tsmiring. Controlling spatiotemporal chaos. *Phys. Rev. Lett.*, 72:2561, 1994.

40. R. Schmitz and W. Zimmermann. Domain pattern and taming of spiral defect chaos in a model for forced convection. submitted, 2003.

41. P. Fromherz. Spatio-temporal patterns in the fluid-mosaic model of membranes. *Biochim. Biophys. Acta*, 944:108, 1988.

42. A. J. Bray. Theory of phase-ordering kinetics. *Adv. Phys.*, 43:357, 1994.